Supplement of Hydrol. Earth Syst. Sci., 24, 2253–2267, 2020
https://doi.org/10.5194/hess-24-2253-2020-supplement

Hydrology and Earth System Sciences
Open Access
EGU

Supplement of

Identifying uncertainties in hydrologic fluxes and seasonality from hydrologic model components for climate change impact assessments

Dongmei Feng and Edward Beighley

Correspondence to: Dongmei Feng (dmei.feng@gmail.com)

Hydrologic model development

The RCM assumes water excess available for surface runoff (e_s) is proportional to precipitation rate (P). The proportion is represented by a coefficient value (e.g., 0 to 100%) and is dependent on land cover, soil and topographic characteristics. The coefficient value is smaller for dry and flat areas with permeable soils and vegetated surfaces, as compared to that for wet and steep areas with more impervious areas (e.g., roads, parking lots, roofs). In this work, a dual runoff-coefficient method is used, which assigns a larger runoff coefficient (C_2) to wet soils (relative soil moisture at upper soil layer $\theta_U \geq$ threshold θ_t) and smaller runoff coefficient (C_1) to dry soils (relative soil moisture $\theta_U <$ threshold θ_t) (Eq. (S1)). The water excess available for subsurface runoff (e_{ss}) is a function of saturated hydraulic conductivity (k_{sat}) and relative soil moisture in lower soil layer (θ_L) (Eq. (S2)).

$$\begin{aligned} e_s &= C_1 \times P \quad for\ \theta_U < \theta_t \\ &= C_2 \times P \quad for\ \theta_U \geq \theta_t \end{aligned} \tag{S1}$$

$$e_{ss} = K_{sat\_all} k_{sat} \times (\frac{\theta_L}{n})^b \tag{S2}$$

where e_s and e_{ss} are water excess available for surface and subsurface runoff, respectively, (m d^{-1}); P is precipitation rate (m d^{-1}); C_1 is dry runoff coefficient; C_2 is wet runoff coefficient; θ_U and θ_L are relative soil moisture at upper and lower soil layer, respectively; θ_t is relative soil moisture threshold differentiating dry and wet soil conditions; k_{sat} is saturated hydraulic conductivity (m d^{-1}); K_{sat_all} is a scaler; b is Clapp-Hornberger parameter and n is soil porosity. C_1, C_2, θ_t and K_{sat_all} are parameters needing calibration.

In the VIC algorithm, surface runoff is generated as infiltration excess where the infiltration rate is characterized by the variable infiltration curve (Wood et al., 1992). In this work, the framework of modified 2-layer VIC model (VIC-2L) (Liang et al., 1996) is used. The water excess available for surface runoff is calculated as shown in Eq. (S3)-(S4). The water excess available for subsurface runoff is a function of soil moisture in lower soil layer (Eq. (S5)), which is a linear function of soil moisture when the soil is relatively dry and quadratic when the soil is close to saturation:

$$e_s = P - z(\theta_s - \theta_U)/\Delta t - z\theta_s \left(max \left| 0, \left[1 - \frac{i_o + P\Delta t}{i_m} \right] \right| \right)^{1+b_i} / \Delta t \tag{S3}$$

$$i_o = i_m \left[1 - (1 - A)^{1/b_i} \right] \tag{S4}$$

$$e_{ss} = \frac{D_S D_M}{W_S \theta_S} \theta_L + \left(D_M - \frac{D_S D_M}{W_S} \right) \left(\frac{max|0, \theta_L - W_S \theta_S|}{\theta_S - W_S \theta_S} \right)^2 \tag{S5}$$

where z is soil depth in upper layers (m); θ_s is relative soil moisture at saturation; i_m is maximum infiltration capacity (m); i_0 is infiltration capacity (m); b_i is infiltration curve parameter; A is the fraction of saturation; D_M is maximum base flow (m d^{-1}); D_S is the fraction of D_M at which the non-linear base flow begins; W_S is the fraction of saturation at which the non-linear base flow occurs; Δt is time step (d). b_i, D_M, D_S and W_S are parameters which need calibration.

In STP algorithm, the surface runoff is generated as saturation excess overland flow (Eq. (S6)). The saturation fraction of the catchment f_{sat} is determined as a function of topographic index (Eq. (S7)-(S8)).

$$e_s = f_{sat} * P \tag{S6}$$

$$f_{sat} = f_{max} * \exp(-0.5\, z_\nabla\, f_{over}) \tag{S7}$$

where f_{sat} is the fraction of saturated area; f_{over} is a decay factor for surface runoff water excess (m^{-1}); z_∇ is groundwater table depth (m); f_{max} is the maximum saturated fraction and is defined as the percent of grid cells in each sub-basin with a topographic index (τ) that is $\geq$ the mean τ determined by averaging all grid cell τ values:

$$\tau = \ln\left(\frac{a}{tan\,(\beta)}\right) \tag{S8}$$

where a is the specific catchment area (i.e.,upslope area per unit contour length) and β is the pixel slope. The specific catchment area a and slope β are calculated for grid cell using the gridded elevation data and the TauDEM tools (Tarboton, 2003).

The water excess available for subsurface runoff is a function of maximum base flow rate and groundwater table depth:

$$e_{ss} = Q_m * \exp(-f_{drain} * z_\nabla) \tag{S9}$$

where f_{drain} is a decay factor for subsurface runoff water excess (m^{-1}), and $Q_m$is the maximum baseflow rate ($m\ d^{-1}$). Water excess for both surface and subsurface runoff are dependent of the groundwater table depth z_∇. Here, the water table depth z_∇ is determined by applying the method used in (Niu et al., 2005), which assumes the water head at depth z is in equilibrium with that at ground water depth z_∇ (Eq. (S10)-(S13)).

$$\varphi(z) - z = \varphi_{sat} - z_\nabla \tag{S10}$$

where $\varphi(z)$ and φ_{sat} are the matric potentials at depth z and at groundwater table depth z_∇ (m). The soil at the groundwater table depth is assumed to be saturated. Based on Clapp-Hornberger relationship (Clapp and Hornberger, 1978), $\varphi(z)$ can be expressed as:

$$\varphi(z) = \varphi_{sat}\left(\frac{\theta(z)}{\theta_{sat}}\right)^{-b} \tag{S11}$$

where $\theta(z)$ and θ_{sat} are soil moisture content at depth z and groundwater table depth z_∇, respectively, b is a Clapp-Hornberger parameter. By substituting Eq. (S10) with Eq. (S11), the soil matric profile at depth z can be expressed as:

$$\theta(z) = \theta_{sat}\left(\frac{\varphi_{sat} - (z_\nabla - z)}{\varphi_{sat}}\right)^{-1/b} \tag{S12}$$

Then, the groundwater table depth (z_∇) can be determined by solving Eq.S13 iteratively.

$$D_\theta = \int_0^{z_\nabla} (\theta_{sat} - \theta(z))dz \tag{S13}$$

where D_θ is the soil moisture deficit, which can be calculated in Eq.S14:

$$D_\theta = \sum_{i=1}^{m} (\theta_{sat} - \theta_i) \nabla z_i \quad \text{(S14)}$$

where θ_i is the soil moisture content at the ith soil layer; ∇z_i is the soil thickness of ith soil layer, m is the number of soil layer, m=2 in this study. In STP algorithm, f_{over}, f_{drain}, Q_m and φ_{sat} are parameters to be calibrated.

$$ET = \min(\mathrm{PET}, \mathrm{W} - \mathrm{W_{min}}) \quad \text{(S15)}$$

where PET is the potential evapotranspiration estimated using the method proposed by Raoufi and Beighley (2017); W is water content in the upper soil layers; W_{min} is the minimum water content in the soil, defined as 0.15× W_s; W_s is soil water content as saturation.

$$K = k_{sat} \times (\frac{\theta_U}{n})^c \quad \text{(S16)}$$

$$D = k_{sat} \times (\frac{\theta_L}{n})^c \quad \text{(S17)}$$

where K is the water flux from the upper soil layer to the lower soil layer (m d^{-1}); and D is the water flux transported from the lower soil layer to the upper soil layer due to diffusion (m d^{-1}).

Plane Routing:

$$\frac{\partial y_s}{dt} + \frac{\partial q_s}{dx_p} = e_s \quad \text{(S18)}$$

$$\frac{\partial y_{ss}}{dt} + \frac{\partial q_{ss}}{dx_p} = e_{ss} \quad \text{(S19)}$$

Channel Routing:

$$\frac{\partial A_c}{dt} + \frac{\partial Q_c}{dx_c} = q_s + q_{ss} \quad \text{(S20)}$$

where y_s and y_{ss} are water depth (or thickness) of surface and subsurface runoff, respectively (m); q_s and q_{ss} are surface and subsurface runoff flow rates per unit width of plane (m^2 s^{-1}); dx_p is the distance step along the plane (m); A_C is the cross section area of flow in the channel (m^2); Q_c is the flow rate in channel (m^3 s^{-1}); dx_c is the distance step along the channel (m); and *dt* is the time step (s).

Uncertainty Analysis

$$SS_{Hyd} = N_{para}N_{GCM}N_{RCP}\sum_{i=1}^{N_{Hyd}}(q_{iooo} - q_{oooo})^2 \quad \text{(S21)}$$

$$SS_{Hyd.para} = N_{GCM}N_{RCP}\sum_{j=1}^{N_{para}}\sum_{i=1}^{N_{Hyd}}(q_{ijoo} - q_{iooo} - q_{ojoo} + q_{oooo})^2 \quad \text{(S22)}$$

$$\begin{aligned} SS_{3.4} = SS_{Total} - (&SS_{Hyd} + SS_{para} + SS_{GCM} + SS_{RCP} + SS_{Hyd.para} \\ &+ SS_{Hyd.GCM} + SS_{Hyd.RCP} + SS_{para.GCM} + SS_{para.RCP} \\ &+ SS_{GCM.RCP}) \end{aligned} \quad \text{(S23)}$$

where q_{iooo} is the average of all simulations from the ith hydrologic model with all combinations of parameter sets, GCMs and RCPs; $q_{ojoo}\ is$ the average of all simulations from the jth parameter set with all combinations of hydrologic models, GCMs and RCPs; q_{ijoo} is the average of all simulations from the ith hydrologic model and jth parameter set with all combinations of GCMs and RCPs. Other terms in Eq. (3) can be calculated similarly using Eq. (S20)-(S21).

$$\delta_e = \frac{1}{6075}\sum_{m=1}^{6075}\frac{SS_e(m)}{SS_{Total}(m)} \quad \text{(S24)}$$

where δ_e is the average fractional effect of term e (i.e, each of 11 terms in Eq. (3)); $SS_e(m)$ is the sum of variance of effect e in the mth subsample, and the $SS_{Total}(m)$ is the total variance in the mth subsample. So in this study, there are 11 δ_e values in total, representing the uncertainty contributions of 11 terms in Eq. (3), with a sum of 1.0.

Probability of estimated changes

Bayesian model averaging (BMA) has been used to infer the probability of a quantity predicted by an ensemble of models(Duan et al. 2007). The BMA scheme can be described as below:
For a predicted quantity variable y (i.e., the discharge), the probability of predicted y, given the observation D = (d_1, d_2, d_3,…, d_t) and model ensemble M = (m_1,m_2,m_3,…, m_K), $p(y|D)$ can be calculated as:

$$p(y|D) = \sum_{k=1}^{K} p(m_k|D) \times p(y|m_k, D) \quad \text{(S25)}$$

where k is the model ID and K is the number of models (i.e., K=3×3×10=90, note, the BMA is performed on historical period (1986-2005), so no RCP is considered); $p(m_k|D)$ is the probability of model k to be the correct model given the observation D; $p(m_k|D)$ is also called the weight of model k which is determined by the model's ability for reproducing the observed values of quantity y; $p(y|m_k, D)$ is the probability that model k generates the prediction of y; here, $p(y|m_k, D)$ is assumed to be normal distribution. If model k predicts a value of f_k, then the probability that model k generates prediction y is normally distributed with a mean $\mu = f_k$ (known) and standard

deviation σ_k (unknown). Therefore, to get the probability of predicted quantity y, the statistics σ_k and the weights $p(m_k|D)$ need to be determined. If we denote $p(m_k|D)$ as w_k and the unknown parameters as θ, then

$$\theta = \{\sigma_k, w_k, k = 1,2,3, \dots K\} \quad \text{(S26)}$$

The optimal θ should maximize the probability of prediction y. If we denote the cost function as $l(\theta)$:

$$l(\theta) = \sum_{k=1}^{K} w_k \times N(y|f_k, \sigma_k) \quad \text{(S27)}$$

To maximize $l(\theta)$, the Expectation–Maximization (EM) algorithm is used. Details on EM can be found in (Duan et al. 2007).

In this study, the annual mean discharge and annual maximum daily discharge are the considered variables. Since these two variables are not normally distributed, a Box-Cox transformation is performed before applying the EM method. Considering the GCMs' predictions are not temporally consistent with reality (i.e., the GCMs' prediction does not have correct timing), the observation and simulation are both ranked from high to low, and then $l(\theta)$ is maximized based on the ranked series. The procedure is as follows:

Step I: Calculate the observed annual mean discharge (or annual maximum daily discharge) at each watershed of interest for the period 1986-2005

Step II: Calculate the simulated annual mean discharge (or annual maximum daily discharge) for each simulation in the ensemble (3×3×10=90 models) for the same period

Step III: Rank the observed and simulated annual mean discharge (or annual maximum daily discharge) in a descending order

Step IV: Calculate the Box–Cox coefficient λ for each watershed by using the *BoxCox.lambda* function in R and transform the quantities by using Eq.S26:

$$z_t = \frac{y_t^{\lambda} - 1}{\lambda} \quad \text{(S28)}$$

Step V: Apply the EM process to the transformed series z_t and estimate the weights and variance of all models

Step VI: Calculate the probability of estimated changes in Qm, Qp and Q_{100} in the future (2081-2100) relative to 1986-2005 using the weights obtained in Step V.

For Q_m, the statistics are:

$$\mu_m = \sum_{k=1}^{K} w_{k,m} \times c_{k,m} \quad \text{(S29)}$$

$$\sigma_m{}^2 = \sum_{k=1}^{K} w_{k,m} \times (c_{k,m} - \mu_m)^2 \quad \text{(S30)}$$

where μ_m and σ_m are the mean and standard deviation of posterior distribution of relative changes in Q_m; $w_{k,m}$ is the weight of model k in terms of Q_m; $c_{k,m}$ is the relative change in Q_m predicted by model k; K is the total number of models, and here it is 90.

For Qp, the statistics are:

$$\mu_p = \sum_{k=1}^{K} w_{k,p} \times c_{k,p} \tag{S31}$$

$$\sigma_p{}^2 = \sum_{k=1}^{K} w_{k,p} \times (c_{k,p} - \mu_p)^2 \tag{S32}$$

where μ_p and σ_p are the mean and standard deviation of posterior distribution of relative changes in Q_p; $w_{k,p}$ is the weight of model k in terms of Q_p; $c_{k,p}$ is the relative change in Q_p predicted by model k.

For Q_{100}, the statistics are:

$$\mu_{100} = \sum_{k=1}^{K} w_{k,p} \times c_{k,100} \tag{S33}$$

$$\sigma_{100}{}^2 = \sum_{k=1}^{K} w_{k,p} \times (c_{k,100} - \mu_{100})^2 \tag{S34}$$

where μ_{100} and σ_{100} are the mean and standard deviation of posterior distribution of relative changes in Q_{100}; $w_{k,p}$ is the weight of model k for Q_p; $c_{k,100}$ is the relative change in Q_{100} predicted by model k. Here, the weights for Q_p are used because Q_{100} is estimated based on the statistics of Q_p series, so it is reasonable to assume that the model having a better ability in reproducing the annual peak discharge should also have a better ability in reproducing the Q_{100}.

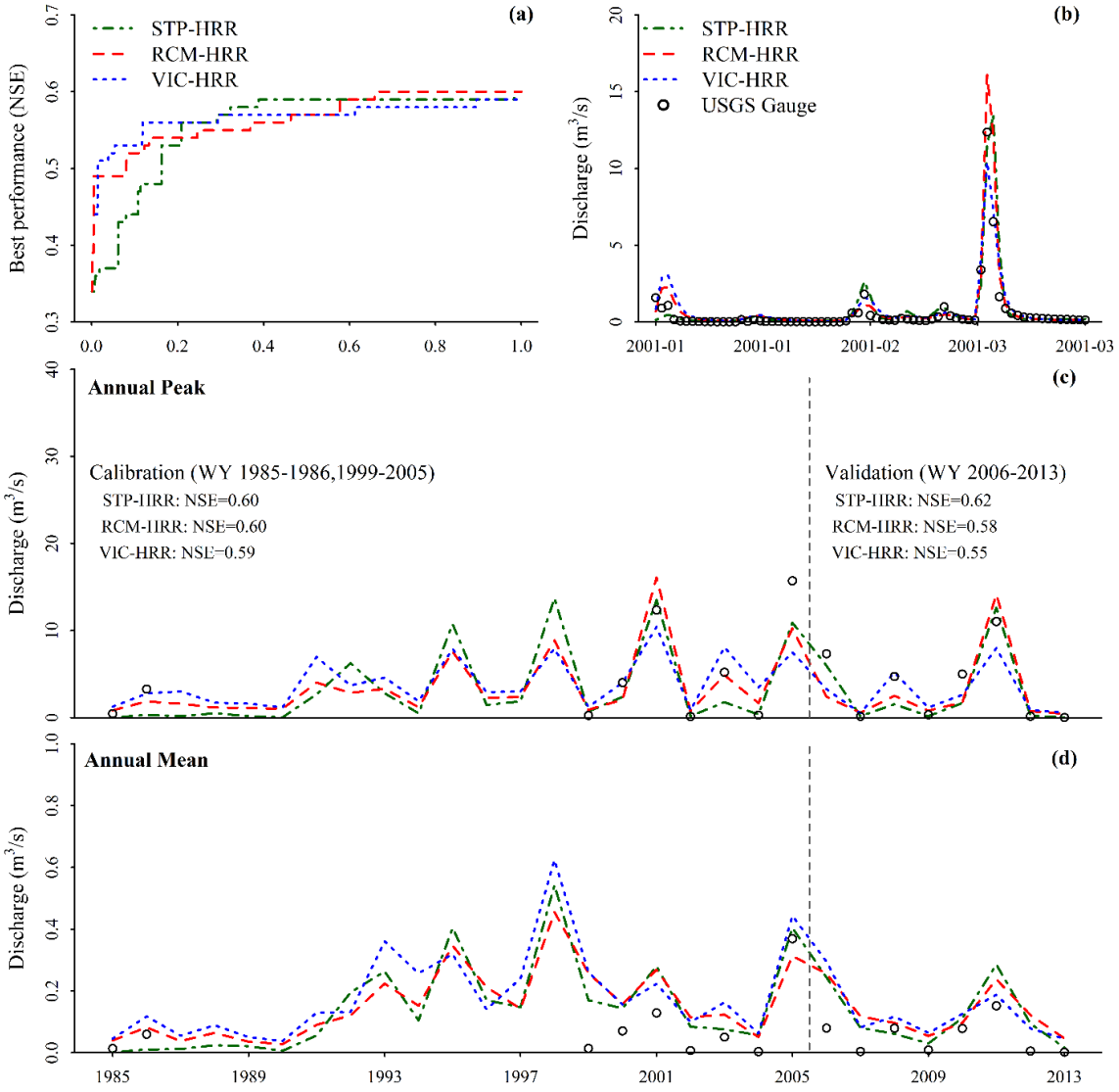

Figure S1. Model performance for calibration and validation periods: (**a**) model performance (represented by NSE) during calibration process, x axis is the normalized calibration progress; (**b**) hydrographs simulated by 3 calibrated models and in situ measurements from USGS gauge; (**c**) simulated annual peak flow during calibration (water year 1985-1986, 1999-2005) and validation (water year 2006-2013) periods as compared with in situ observation; texts indicate model performance (i.e., NSE) in reproducing historical hydrographs for both periods; and (**d**) simulated and observed annual mean flow during calibration and validation periods. These results are for Mission Creek watershed (USGS gauge NO. 11119745).

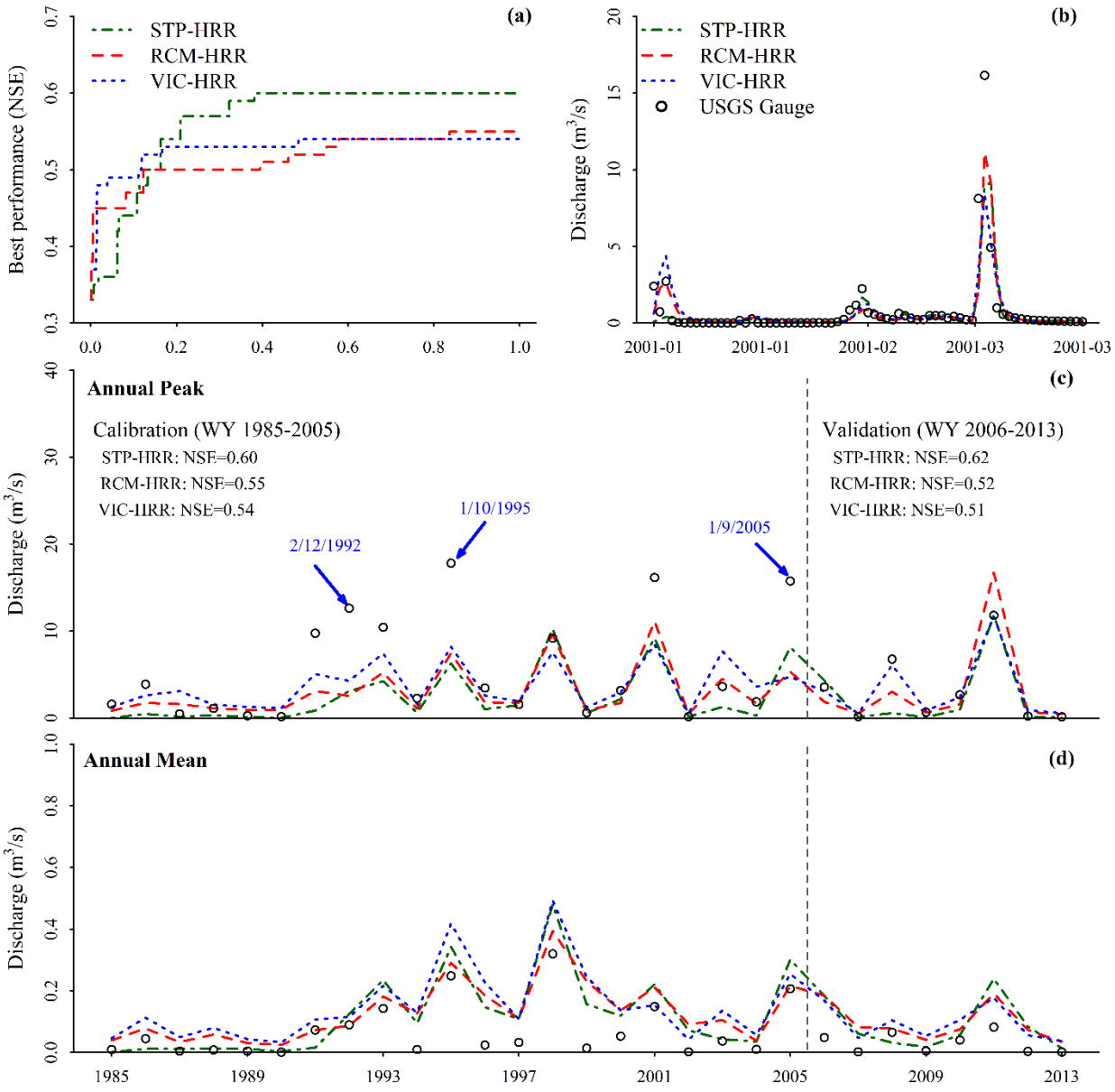

Figure S2. Model performance for calibration and validation periods: (**a**) model performance (represented by NSE) during calibration process, x axis is the normalized calibration progress; (**b**) hydrographs simulated by 3 calibrated models and in situ measurements from USGS gauge; (**c**) simulated annual peak flow during calibration (water year 1985-2005) and validation (water year 2006-2013) periods as compared with in situ observation; texts indicate model performance (i.e., NSE) in reproducing historical hydrographs for both periods; the points highlighted in blue arrows indicate the events which were not reproduced by models probably due to the input (i.e., precipitation) bias; and (**d**) simulated and observed annual mean flow during calibration and validation periods. These results are for Maria Ygnacio Creek at Goleta (USGS gauge NO. 11119940).

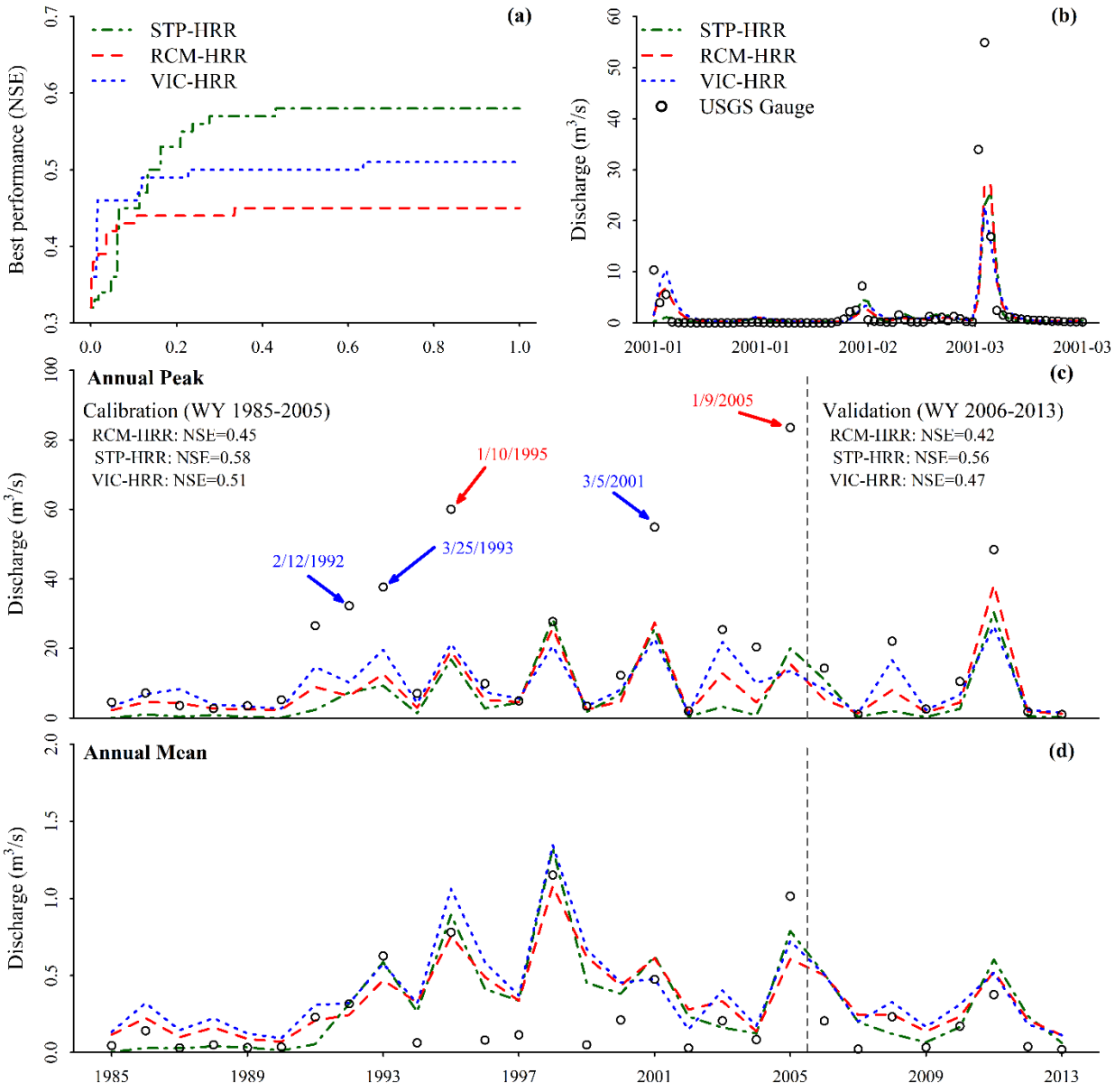

Figure S3. Model performance for calibration and validation periods: (**a**) model performance (represented by NSE) during calibration process, x axis is the normalized calibration progress; (**b**) hydrographs simulated by 3 calibrated models and in situ measurements from USGS gauge; (**c**) simulated annual peak flow during calibration (water year 1985-2005) and validation (water year 2006-2013) periods as compared with in situ observation; texts indicate model performance (i.e., NSE) in reproducing historical hydrographs for both periods; the points highlighted in red arrows indicate the events which were not reproduced by models due to the input (i.e., precipitation) bias; the points highlighted in blue arrow are similar to those in red but at a lower probability; and (**d**) simulated and observed annual mean flow during calibration and validation periods. These results are for Atascadero Creek at Goleta (USGS gauge NO. 11120000).

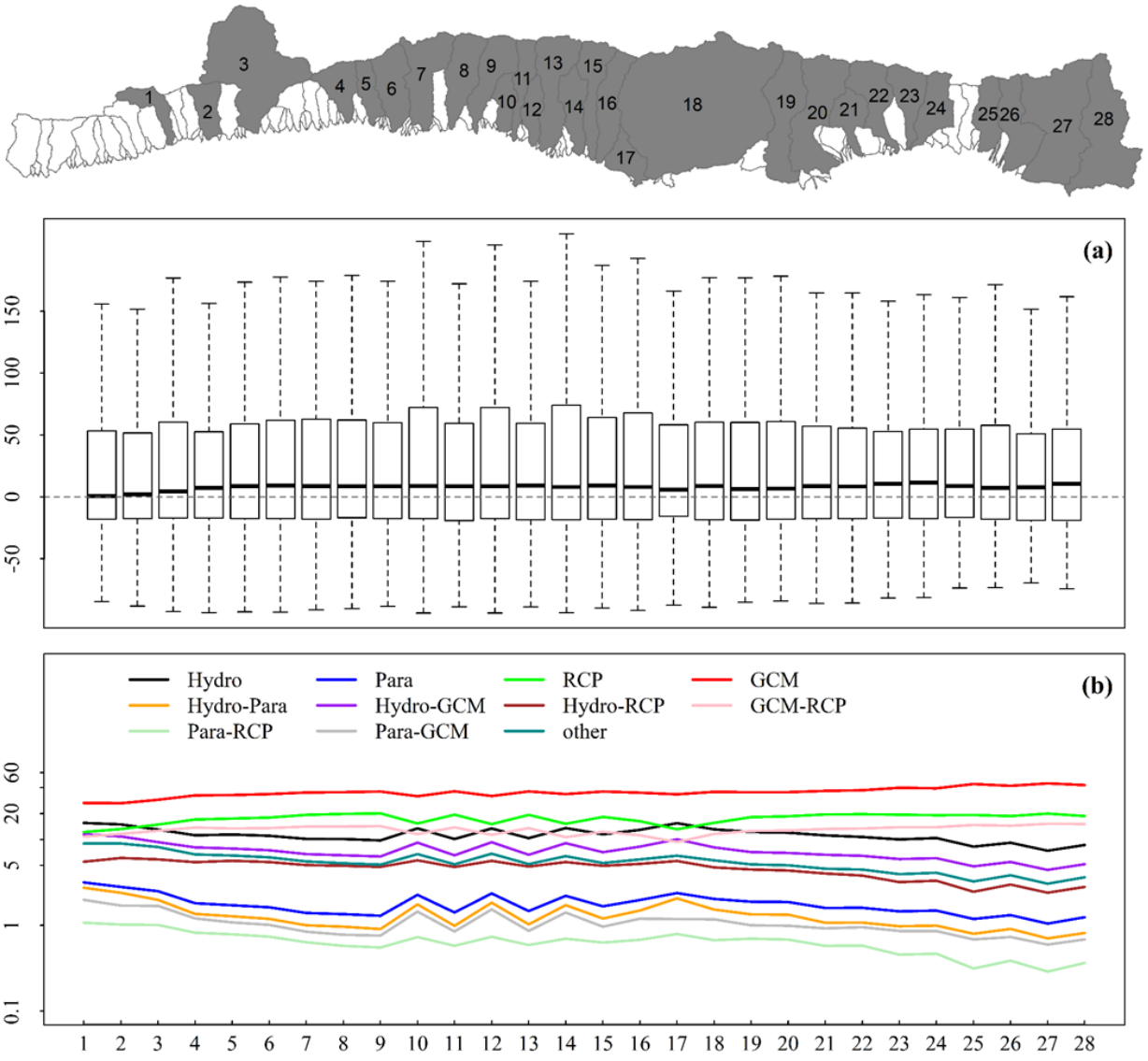

Figure S4. (a) Projected relative changes (%) in annual mean discharge (Q_m) in the major SBC watersheds (indicated by the grey watersheds in the map) during 2081-2100 as compared to historical period (1986-2005); each bar depicts relative changes in minimum, maximum, median, 1st and 3rd quartiles for the ensemble outputs; bars from left to right spatially corresponding to watersheds from west to east. For clarity, only watersheds with drainage areas larger than 7 km^2, which account for roughly 83% of the study area, are shown. (b) Relative sources (%) of the uncertainties in the projected changes at each of these watersheds; the category "other" is the uncertainty from the 3rd and 4th orders of interactions between the 4 major sources (i.e., GCMs, RCPs, Hydrologic models, denoted by "Hydro" and parameters denoted by "Para")

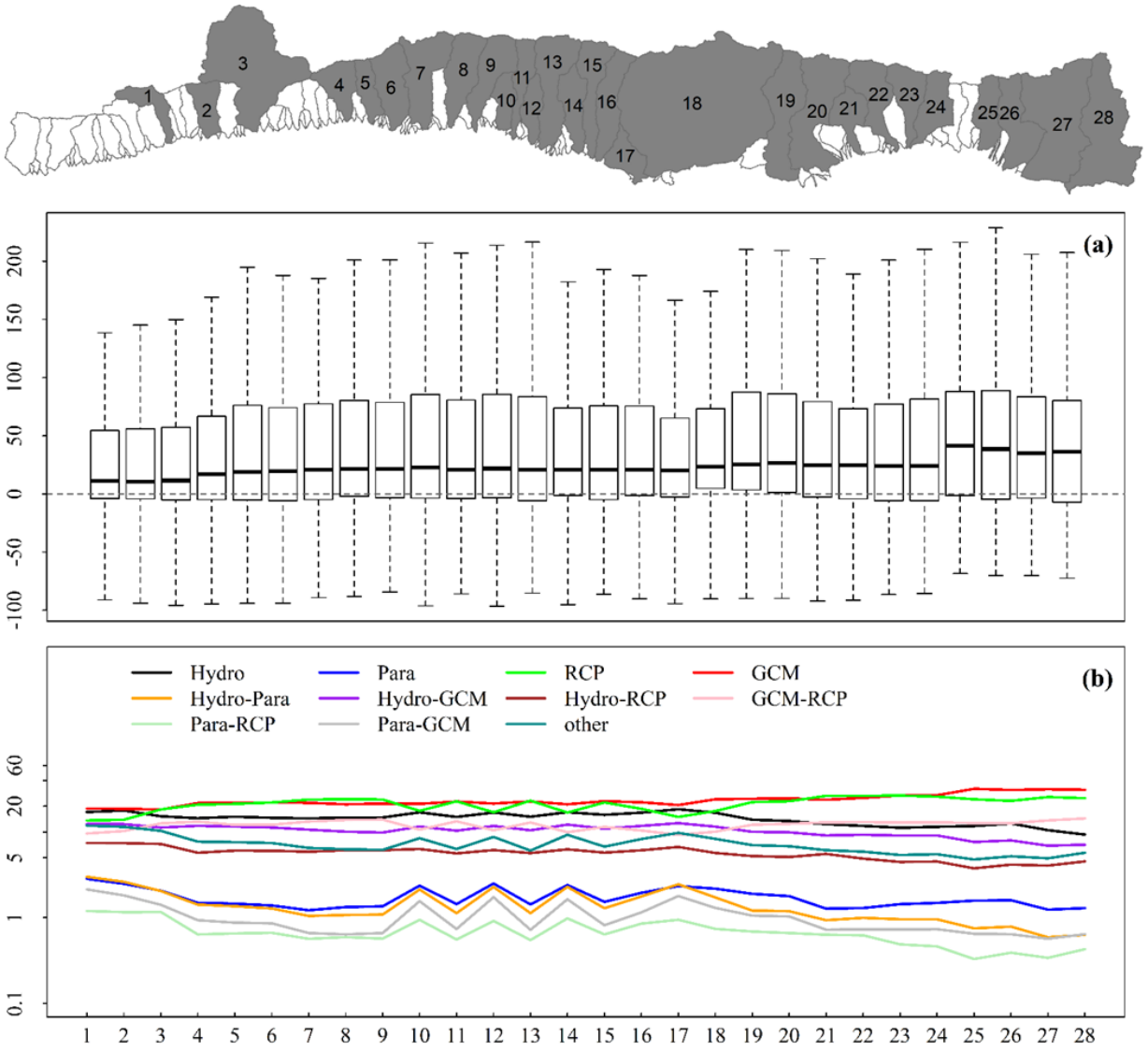

Figure S5. (a) Projected relative changes (%) in annual peak discharge (Q_p) in the major SBC watersheds (indicated by the grey watersheds in the map) during 2081-2100 as compared to historical period (1986-2005); each bar depicts relative changes in minimum, maximum, median, 1st and 3rd quartiles for the ensemble outputs; bars from left to right spatially corresponding to watersheds from west to east. For clarity, only watersheds with drainage areas larger than 7 km^2, which account for roughly 83% of the study area, are shown. (b) Relative sources (%) of the uncertainties in the projected changes at each of these watersheds; the category "other" is the uncertainty from the 3rd and 4th orders of interactions between the 4 major sources (i.e., GCMs, RCPs, Hydrologic models, denoted by "Hydro" and parameters denoted by "Para")